

## 6.4 GHZ ACOUSTIC SENSOR FOR IN-SITU MONITORING OF AFM TIP WEAR

Tiffany J. Cheng<sup>1</sup>, Jun Hyun Han<sup>2</sup>, Michael Ziwiisky<sup>2</sup>, Chung Hoon Lee<sup>2</sup> and Sunil A. Bhawe<sup>1</sup>

<sup>1</sup>Cornell University, Ithaca, NY, USA

<sup>2</sup>Marquette University, Milwaukee, WI, USA

### ABSTRACT

This paper demonstrates an acoustic sensor that can resolve atomic force microscopy (AFM) tip blunting with a frequency sensitivity of 0.007%. The AFM tip is fabricated on a thin film piezoelectric aluminum nitride (AlN) membrane that is excited as a film bulk acoustic resonator (FBAR). We demonstrate that cutting 0.98  $\mu\text{m}$  off of the tip apex results in a resonance frequency change of 0.4MHz at 6.387GHz. This work demonstrates the potential for in-situ monitoring of AFM tip wear.

### INTRODUCTION

#### Motivation

The shape and diameter of the tip apex is a crucial factor in AFM and high precision tip-based nanoscale fabrication. Over continual use, an AFM tip becomes worn and its tip diameter increases, leading to resolution degradation and information distortion. Current methods of characterizing tip shape include running the tip over a separate test structure.[1][2] Another method employed is 3D STM imaging of the tip.[3] Both methods have high accuracy, but are time-consuming.

#### Principle of Operation

We propose launching an acoustic wave in the AFM tip at GHz frequencies (sub-micron wavelengths), thus enabling an in-situ and non-contact monitoring of nanometer changes at the tip end. Acoustic transmission into a tip for ultrasonic

imaging and microscopy has previously been demonstrated at 1.44MHz and at 135MHz with a bulk piezoelectric transducer bonded to the base of a tip.[4][5] We have fabricated a similar structure, except with thin-film aluminum nitride as a high-bandwidth transducer. FBAR resonators have large effective mass, rendering them poor absolute mass sensors. Instead, we intend to measure frequency shifts in the acoustic standing wave that can be sustained inside the AFM tip itself.

Tip blunting can cause both positive and negative frequency shifts, as demonstrated in Figure 1. For “Blunt 1,” neither the mode with slightly higher frequency  $f_1$ , nor a higher harmonic of  $f_2$  fits into the blunted structure. Instead, a mode with slightly longer wavelength is excited, causing a small negative frequency shift to  $f_3$ . Conversely, cutting off an amount that is small relative to the original wavelength  $\lambda_2$ , as shown in “Blunt 2,” results in a small positive frequency shift to  $f_1$ .

### FABRICATION

For initial demonstration of the concept, the tip was fabricated on a membrane instead of a cantilever. This renders the tip incapable of actually being used in AFM mode, but enables easy RF routing and characterization.

Figure 2 shows the fabrication process. Starting with an SOI wafer, 200nm of thermal oxide is grown followed by 500nm of LPCVD silicon nitride. Platinum (200nm thick) is sputtered and patterned by liftoff to form the bottom electrodes on the device layer of the SOI wafer. AlN (224nm thick) is then deposited in an RF magnetron sputtering tool by OEMGroup. The AlN film is patterned to create access to the bottom electrodes. The top electrode is created by evaporating 200nm of aluminum and patterning by liftoff. The tip is formed through backside processing of the SOI wafer. The handle of the SOI wafer is first removed by etching in wet potassium hydroxide solution (KOH). The buried oxide layer is then used as an etch mask for the subsequent KOH etch to form the tip in the device layer. The most challenging part of the process is protecting the AlN during the hours-long KOH etch to remove the SOI handle. The silicon nitride and silicon dioxide layers protect the transducer from below. The transducer-side is protected by a glass cap that is anodically bonded to the SOI wafer. Hollowed-out cavities in the glass are aligned with the die. (Figure 1, part (f)) The glass cap serves the dual purpose of acting as a KOH etch mask as well as a carrier wafer for the membrane that is left after the SOI handle is removed.

After tip formation on the device layer, the transducer-side electrodes are accessed by breaking the glass cavities enclosing each die, yielding the final structure shown in

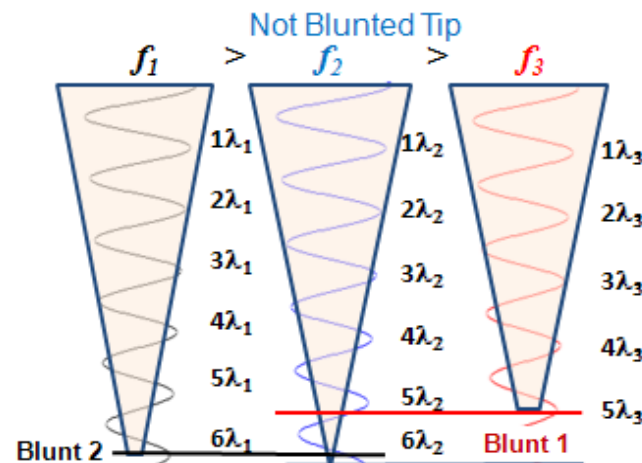


Figure 1: Consider longitudinal overtone modes in a tip with free boundary conditions on the ends. The tip undergoing “Blunt 2” will be excited in a mode with slightly shorter wavelength and slightly higher frequency. For “Blunt 1,” a mode with longer wavelength and slightly lower frequency is preferentially excited.

## Process Flow A – A'

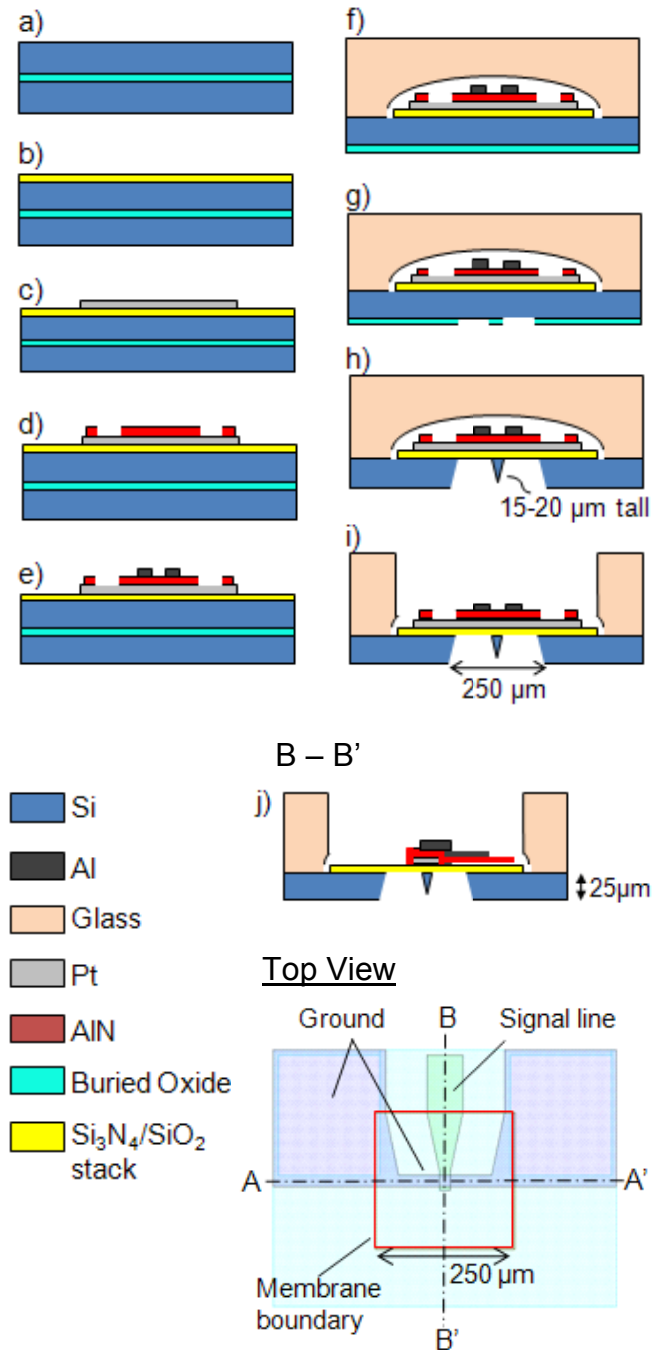


Figure 2: (a) SOI wafer (b) Thermal oxidation, then LPCVD low-stress  $\text{Si}_3\text{N}_4$  (c) Deposit bottom Pt electrode (d) Sputter and wet etch AlN (e) Deposit top Al electrode (f) Reactive ion etch (RIE)  $\text{Si}_3\text{N}_4$  and  $\text{SiO}_2$  to expose Si for anodic bonding of glass cap (g) KOH etch SOI handle, then RIE buried oxide layer (h) KOH etch device layer to form tip and remove oxide mask (i) Break glass cap to access electrodes. (j) B – B' cross-section of the final device

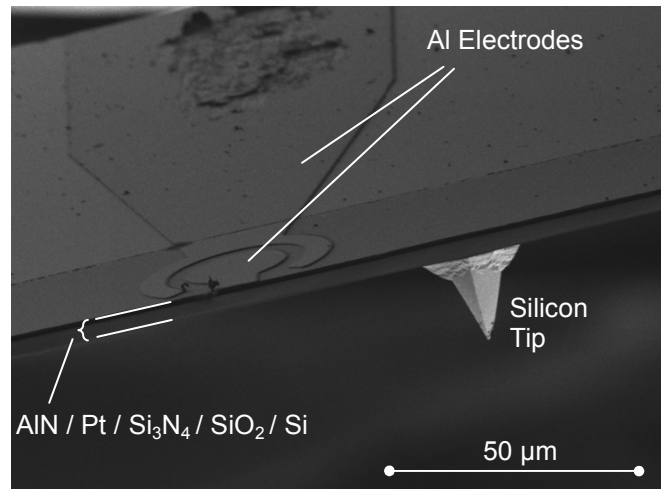


Figure 3: Cross-sectional SEM the silicon AFM tip with FBAR fabricated on top. This SEM is of a 2-port device.

Figure 2, parts (i) and (j). Only the  $\text{SiO}_2/\text{Si}_3\text{N}_4$  stack exists between the transducer and the tip, facilitating strong acoustic transmission into the tip. To maintain structural strength of the wafer, the thin membrane areas are bound by  $\sim 25\mu\text{m}$ -thick silicon. The tip is therefore easily accessible to blunting, which will be described further in the experimental section. GSG pads are placed close to the tip to minimize electrical resistance.

In the device fabrication, the glass anodic bonding caused the hollowed cavities to pressurize, causing the die membrane to deform after the handle is removed by KOH. Subsequently, photolithography on the curved membrane surface resulted in slight misalignment of the tip from the metal-AlN-metal stack. (Figure 3) However, the AlN film still extends over the misaligned tip. Therefore, the strong acoustic signal existent in the AlN during RF excitation will couple into the tip.

## EXPERIMENTAL RESULTS

The tip was blunted using focused ion beam, which enables precise control over the tip apex removal. The structure was first angled perpendicular to the ion beam, and then tilted  $4^\circ$  to  $5^\circ$  until the tip end emerged over the surrounding silicon walls. (Figure 4) The amount cut off was chosen to be from the end of the tip to the top of the silicon trench. (Figure 5)

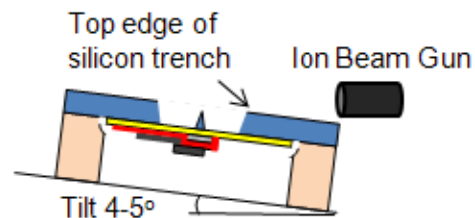


Figure 4: Orientation of sample when blunting the tip using focused ion beam.

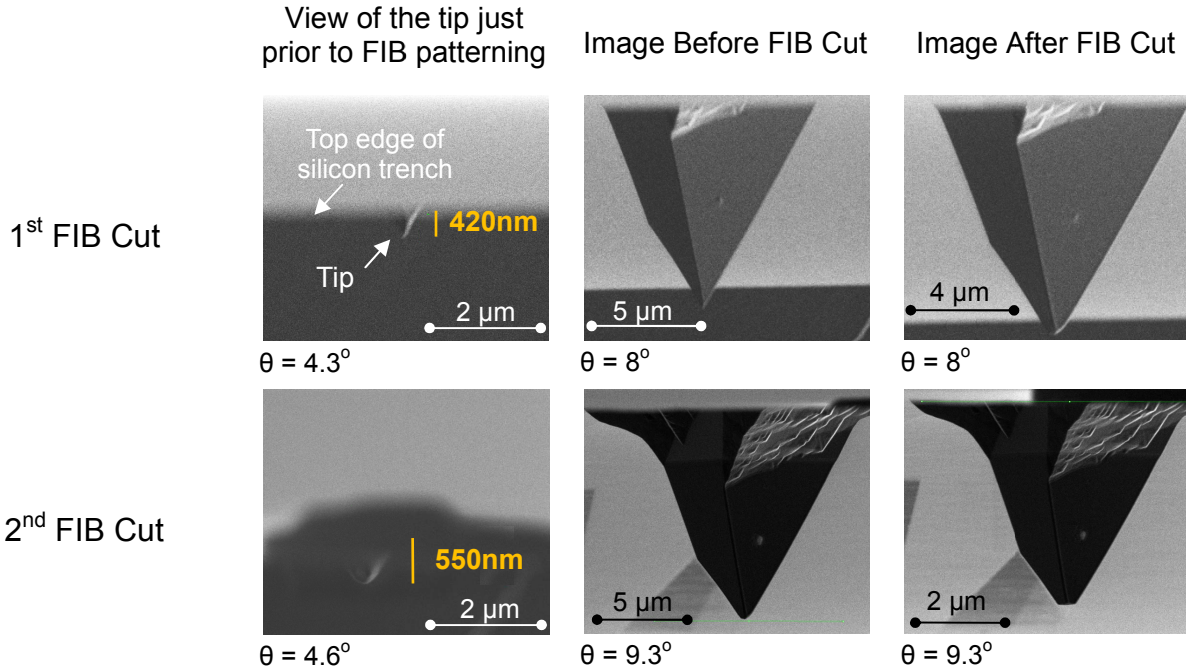


Figure 5: Focused ion beam (FIB) images taken of the same tip for 2 cuts. The tip was first placed perpendicular to the ion beam and then angled  $\theta$  degrees (refer to Figure 4). The height (measured at angle  $\theta$ ) of the amount cut off is indicated in yellow. The first column of images shows how FIB patterning took place with the tip end just visible over silicon trench wall. The last two columns show the blunt amount in relation to an expanded vertical view of the tip.

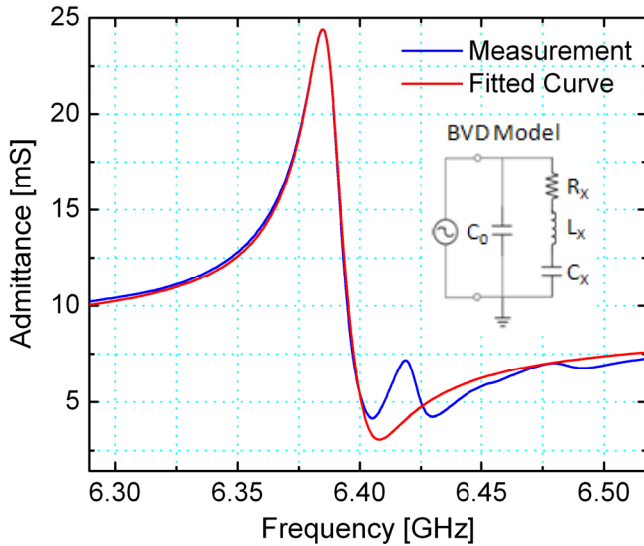


Figure 6: Resonance response taken on the device before any blunting. At 6.39GHz, the extracted coupling coefficient  $kt^2$  is 0.6% and quality factor is 443.

The admittance spectrum was measured in air before and after tip blunting using an Agilent E8364B network analyzer. It is difficult to determine the frequency shift directly from the admittance plots because the change is very small. As shown in Figure 7, the difference in amplitude of the peaks before and after blunting further complicates determination of the frequency shift.

Therefore, the resonance frequency was determined by fitting the data to a Butterworth Van Dyke (BVD) model. (Figure 6) During measurement, the chips were placed with the tip facing down, while RF probes were landed on top. To protect the tip, the chip was placed on a chuck that only supported the chip at the edges.

Several precautions were taken to eliminate other factors that could cause a resonance frequency shift. To account for drift of the device over time, measurements were taken on a reference device at the same time as the device being blunted. The reference device is an FBAR with no tip and is physically located next to the device being blunted. Both devices experience the same environmental conditions, with the exception of tip blunting. During measurement, stress may be induced in the edge-supported 25 $\mu$ m-thick membrane from landing RF probes. To minimize large variations in this stress, care was taken to land the probes in the same location before and after tip blunting. Furthermore, several measurements were taken on the same device each time the tip was blunted. The mean of the extracted resonance frequencies was used to determine frequency shifts due to the tip blunting.

Table 1 details the resonance frequency progression of the 1-port device in Figure 5 and a reference device. Measurements were taken before any cut and after the second cut. (Figure 7) The blunt amounts in Table 1 have been corrected for the angle at which they were measured. After subtracting the frequency shift of the reference device, the net frequency change experienced by the blunted device

Table 1: Extracted Resonance Frequencies

Tip Blunting	Blunted Tip Device		Reference Device	
	Mean Resonance Frequency (GHz)	# of Data Points	Mean Resonance Frequency (GHz)	# of Data Points
0 $\mu\text{m}$	6.38745	6	6.31978	3
0.98 $\mu\text{m}$	6.38655	5	6.31932	5

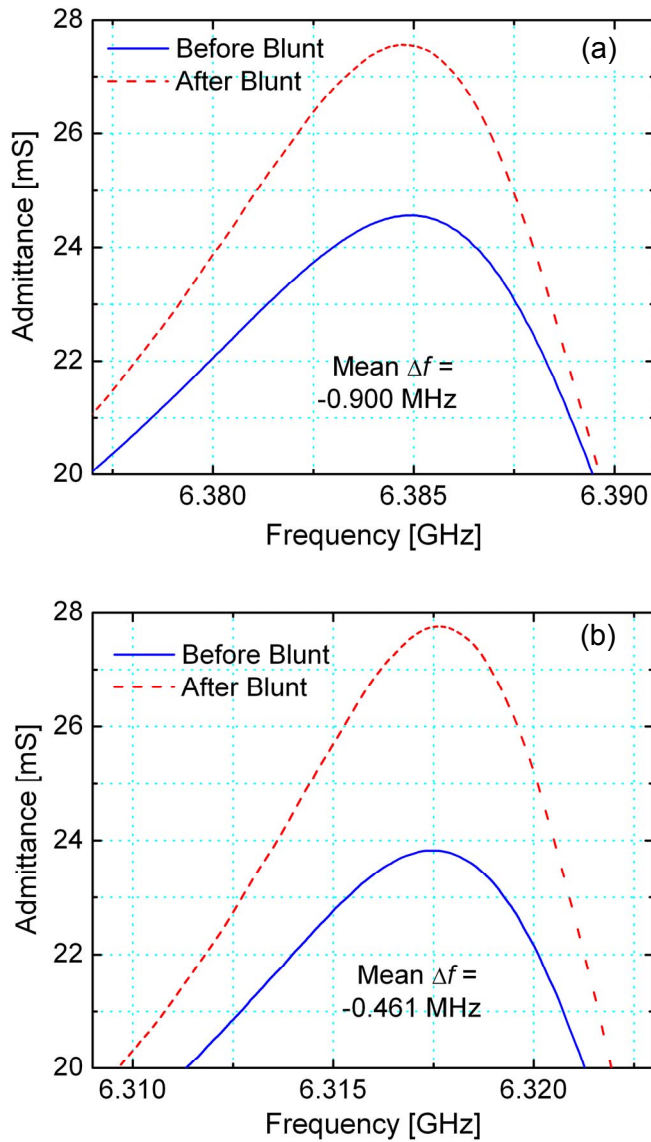


Figure 7: Comparison of admittance measurements taken before and after blunting for the device (a) and reference (b). Plots are zoomed to the very apex of the resonance peak.

after blunting 0.98  $\mu\text{m}$  is  $-439,141$  kHz at 6.387 GHz. The negative sign of the frequency shift is consistent with the theory presented in Figure 1. Assuming a Young's modulus of silicon to be 170GPa and the density to be 2.33  $\text{g/cm}^3$ , the wavelength in silicon at 6.387GHz is 1.34 $\mu\text{m}$ . The total blunt of 0.98 $\mu\text{m}$  shortens the tip by 0.73 $\lambda$ , which is just short of 0.75 $\lambda$  and therefore corresponds to "Blunt 1" in Figure 1.

## CONCLUSION

A thin-film, high bandwidth transducer on top of an AFM tip has been fabricated and measured. Shifts in the resonance frequency after the tip has been shortened indicate that the device can resolve sub-micron blunting of the tip apex. With this low frequency resolution and a sustaining oscillator circuit, we can not only measure tip wear, but also implement a tip-based nanosecond ultrasonic source.

## ACKNOWLEDGMENTS

The authors would like to thank the Tip-Based Nanofabrication program from DARPA/MTO (Contract#: N66001-08-1-2074) and NSF for funding this work. We also acknowledge OEMGroup for providing the AlN thin films, and Dr. Matteo Rinaldi and the PMA NS lab at the University of Pennsylvania for their considerable advice on the AlN transducer fabrication process.

## REFERENCES

- [1] Y.Wang and X.Chen, "Carbon nanotubes: A promising standard for quantitative evaluation of AFM tip apex geometry," *Ultramicroscopy*, vol.107, pp.293-298, 2007
- [2] J.P. Spatz, S.S. Sheiko, and M. Moller, "Shape and quality control of modified scanning force microscopy tips," *Ultramicroscopy*, vol. 75, pp.1-4, 1998
- [3] Zyvex Labs, personal communication
- [4] B.T. Khuri-Yakub, S. Akamine, B. Hadimioglu, H. Yamada, and C.F.Quate, "Near Field Acoustic Microscopy," *Proc. of SPIE*, vol. 1556, pp.30-39, 1991
- [5] K. Uozumi and K. Yamamuro, "A Possible Novel Scanning Ultrasonic Tip Microscope," *JJAP*, vol. 28, no.7, pp.L1297-L1299, 1998